Colloids and Surfaces B: Biointerfaces 87 (2011) 361–368

Contents lists available at ScienceDirect

Colloids and Surfaces B: Biointerfaces

journal homepage: www.elsevier.com/locate/colsurfb

Effects of chemical and physical parameters in the generation of microspheres by hydrodynamic flow focusing

Thomas Schneider[a,b,*], Glenn H. Chapman[c], Urs O. Häfeli[a]

[a] Faculty of Pharmaceutical Sciences, The University of British Columbia, 2146 East Mall, Vancouver, B.C. V6T 1Z3, Canada
[b] Department of Chemistry, University of Washington, Bagley Hall 012, Seattle, WA 98195, USA
[c] School of Engineering Science, Simon Fraser University, Burnaby, B.C. V5A 1S6, Canada

ARTICLE INFO

Article history:
Received 29 December 2010
Received in revised form 20 April 2011
Accepted 22 May 2011
Available online 27 May 2011

Keywords:
Hydrodynamic flow focusing
Poly(lactide-co-glycolide)
Microspheres
Biodegradable polymers
Droplet and particle generation
Solvent composition

ABSTRACT

Hydrodynamic flow focusing is a seminal, easy-to-use technology for micro- and nanodroplet generation. It is characterized by the co-axial focusing of two (or more) immiscible liquid streams forced through a small orifice. In this method, the outer continuous phase has a much higher flow velocity than the inner disperse phase. While passing through the orifice, the prevailing pressure drop and shear stress force the inner phase to break up into uniform droplets. Using a biodegradable poly(lactide-co-glycolide) (PLGA) polymer solution as the disperse phase, monodisperse and user-defined polymer micro- and nanospheres can be generated. Here we present a consecutive parameter study of hydrodynamic flow focusing to study the effect of chemical and physical parameters that effect the dispersity of the droplets generated in the 1–5 μm range. The parameter study shows the applicability and challenges of hydrodynamic flow focusing in the preparation of biodegradable microspheres. Applications for microspheres made with this method can be found in the medical, pharmaceutical and technical fields.

1. Introduction

The mass production of uniform and size-defined micro- and nanoparticles is a challenge in many fields, and especially in the pharmaceutical industry. Here, the production of particles that are not only biodegradable, but are also of small enough size to be used for *in vivo* drug delivery and large enough to remain sufficiently long in the blood stream (*e.g.*, particles in the 1–5 μm diameters) gains more and more importance [1]. Current methods lack the ability to produce such particles with a narrow size distribution and in a single step approach. In order to achieve particle batches with similar particle sizes, many technologies (*e.g.*, spray drying, milling techniques, or oil-in-water emulsion technologies) require additional methods to reduce the particle size to a range demanded by the customer (*i.e.*, sieving, capillary electrophoresis, size-exclusion chromatography, or SPLITT fractionation) [2–6]. The use of additional methods for particle size reduction and, as a result, the significant increase in costs is justified by the demand of such particle batches.

In drug delivery applications, particle size has two important consequences. Firstly, it can determine the final site of particle accumulation within the body and secondly, it can effect the release rate and release profile of a drug and thereby its therapeutic efficacy. Employing micro- and nano-particles which are uniform in size will allow for maximal control over particle biodistribution, followed by a precisely regulated drug release [7,8].

To meet the demand for uniform size, various particle preparation methods have been proposed and tested. In batch crystallization, a traditional method of direct drug particle generation, homogeneous size is achieved after the product undergoes labour- and cost-intensive processing steps, such as filtration/sieving, drying, and micronization (*e.g.*, by milling). Despite these procedures, the powders produced are often of poor quality, exhibit broad distributions in shape and size, and often contain electrostatic charges which were introduced during the milling process [9]. More control is gained over size, shape, and active component distribution (*e.g.*, drug) with the methods of spray drying [10], solvent evaporation/emulsification [11,12], phase separation [11,13], and rapid freeze drying [14]. An additional advantage of these methods for the preparation of drug-loaded microspheres, and particularly of the freeze drying method, is their high throughput. None of the methods mentioned, however, allow for the production of monosized particles in a single step approach, and the size can be adjusted in general only over a very limited range.

A particle preparation method that gives rise to uniform, monodisperse polymeric micro- and nanospheres in a single step is flow focusing [15]. In hydrodynamic flow focusing, two or more phases of liquid are co-axially focused and then forced through a small orifice (Fig. 1). The flow rate of the outer phase, called the

* Corresponding author at: Department of Chemistry, University of Washington, Seattle, WA 98195, USA. Tel.: +1 206 543 6665.
E-mail address: tschneid@uw.edu (T. Schneider).

0927-7765/$ – see front matter © 2011 Elsevier B.V. All rights reserved.
doi:10.1016/j.colsurfb.2011.05.040

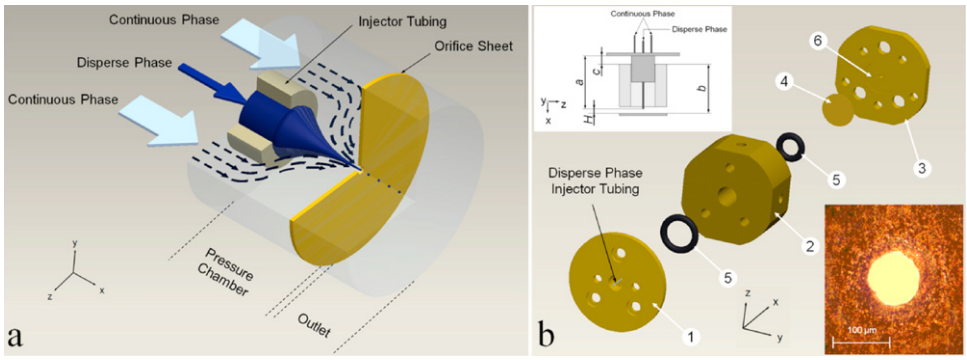

Fig. 1. (a) Flow focusing principle. The disperse phase (*DP*) is injected into a sheath stream of the continuous phase (*CP*) and forced through a small orifice. High shear stress and the prevailing rapid pressure drop at the orifice result in a break-up of the *DP* into droplets. (b) Design of the flow focusing apparatus used in the study showing (1) an injector plate with implemented injectors for the *CP* and the *DP*, as well as alignment holes to enable the positioning relative to the channel body (2; *x*-direction) using a standard caliper. The bottom plate (3) has similar position holes as well as a notch (6) for the orifice sheet (4). Rubber O-rings (5) help sealing the channel body with the injector and bottom plate. The insets in (b) show the relevant distances (a, b, c) allowing a precise positioning of the *DP* injector tip relative to the orifice (distance *H*). Also shown is a light microscopy image of one of the orifices prepared by a laser ion beam.

continuous phase (*CP*), exceeds that of the inner disperse phase (*DP*), typically by ten to thousand times. The *DP* is thus forced into a narrow jet and focussed at the orifice. Due to the rapid change in pressure from the pressure chamber to the outlet and the prevailing shear stress, the jet breaks up into droplets after passing the orifice. In order to generate drug-containing polymer particles, the *DP* must contain the polymer(s) and drug(s). Immediately after droplet formation, the *DP* solvent starts to evaporate or is extracted by the surrounding fluid, leaving behind solid micro- or nanospheres. Maintaining precise control over the initial droplet size allows the formation of close to monosized particles.

Research on flow focusing and droplet disintegration is not a new topic. Studies with different orifice arrangements were already conducted in the late 19th century by Lord Rayleigh [16,17]. Applications of flow focusing, however, have only matured during the past 20–30 years, alongside the advances in microfabrication and measurement technology. A well-established patented flow focusing technology which involves the mass production of droplets on demand with defined size is ink jet printing [18]. Flow cytometry also employs a similar flow focusing technology to focus cells or particles in a single-file fashion [19,20]. More recent applications of the flow focusing method include not only the controlled preparation of bubbles, droplets, and capsules [21,22], but also the preparation of uniform polystyrene microspheres, some of which contain fluorochrome dyes [23,24]. So far, however, most applications focused on polymers that had either short chain lengths, were unbranched, or non-biodegradable.

The use of biodegradable polymers with the flow focusing method would allow the microsphere generation of specific size, which could be used *in vivo* and would then slowly disintegrate without toxic side effects. Recent studies have shown the successful preparation of biodegradable drug loaded particles for drug delivery studies with diameters on the order of 8–10 μm [1,25]. Here we investigate the potential of flow focusing for the preparation of biodegradable microspheres, with diameters below 5 μm. Particles of such a small size will improve the drug delivery when compared to larger particles as a result of better distribution in small blood capillaries. As a biodegradable polymer material, poly(lactide-co-glycolide) (PLGA) was used as it allows for controlled (slow) drug release, is biocompatible and non-toxic, and can remain in the body after therapy since it degrades slowly over time [26]. In this work, we evaluated the influence of various parameters on the final particle size and their size distribution. The parameters included fluid flow velocities and ratios, injector position and orifice size, as well as the liquid properties and polymer concentrations. While the main focus is not the generation of uniform monodisperse particles, the current work can be used as a guide in the optimization of process parameters to achieve better uniformity and reduce dispersity in microspheres generated by this method.

2. Materials and methods

2.1. Sources of materials

PLGA (85/15, intrinsic viscosity 0.61, MW 24 kDa, Lot# D96056) was purchased from Durect Corp. (Pelham, AL, USA), polyvinyl alcohol (PVA; 87–89% hydrolized, MW 13 kDa–23 kDa) from Sigma Aldrich Ltd. (Oakville, ON, Canada), dichloromethane and chloroform from Fisher Scientific (Ottawa, ON, Canada). All chemicals were of reagent grade and were used as received. 2 Ton® Clear Epoxy glue was from ITW Devcon (Danvers, MA, USA). Corrosion resistant TEFZEL tubing in various dimensions was purchased from Upchurch Scientific (Oak Harbor, WA, USA). Standardized stainless steel tubing was purchased from EFD Inc. (East Providence, RI, USA).

2.2. Design and fabrication of the flow focusing apparatus

The flow focusing apparatus was designed using ProEngineer software (ProEngineer Wildfire, PTC, Needham, MA, USA) and subsequently fabricated from brass in a local machine shop (UBC, Department of Mechanical Engineering). The apparatus consisted of three major sections: a pressure chamber, a bottom plate, and an injector holder (see Fig. 1b). The internal dimensions of the pressure chamber were 6.0 mm in diameter and 10.0 mm in length. The stainless steel tubings were glued into the injector holder (2 Ton® Clear Epoxy) to form four radial, equally distributed injectors for the *CP* (25G; OD = 0.508 mm, ID = 0.254 mm) and one central injector for the *DP* (26G; OD = 0.4572 mm, ID = 0.254 mm). The *CP* tubings were combined and glued into TEFZEL tubing (0.254 mm ID, 1.5875 mm OD).

The *DP* injector was set in the injector holder so that it protruded from the flow focusing apparatus body (see inset in Fig. 1b, $a = 16.1$ mm) thereby accommodating a rubber seal (O-ring) that was used for later adjustment of the injector's position relative to the orifice in the *x*-direction. The stainless steel tubing of the *DP* injector was connected to TEFZEL tubing by press-fit. The tubing length was minimized to reduce void volume. The orifice was manufactured at Simon Fraser University, Burnaby, Canada using a focused 5 W argon ion laser beam, capable of drilling holes of diameters as small as 1 μm. The resulting orifice had a diameter of 100 μm in a 50 μm thick brass sheet (Fig. 1b). The pre-cut round orifice brass sheet was fixed and optically centered in the bottom

Table 1
Summary of the investigated parameters.

Parameter study	PLGA solvent composition [% $CHCl_3$/% CH_2Cl_2]	PLGA conc. [wt%]	Total flow rate [ml/min]	Flow rate ratio [Q_{DP}:Q_{total}]	Injector position [mm]
PLGA solvent composition	100/0 75/25 50/50 25/75 0/100	10	8.0	1:1000	1.0
PLGA concentration	100/0	1 5 10 15 20	8.0	1:1000	1.0
Flow rate	100/0	10	4.0 6.0 8.0	1:1000	1.0
Flow rate ratio	100/0	10	8.0	1:100 1:500 1:1000 1:2000	1.0
Injector position	100/0	10	8.0	1:1000	0.5 1.0 1.5

Constant parameters: $D_{orifice}$ = 100 μm; continuous phase = 2 wt% PVA; $CHCl_3$ – chloroform; CH_2Cl_2 – dichloromethane.

plate's notch (number 6 in Fig. 1b) and the plate-orifice assembly sealed on the bottom of the pressure chamber using a rubber O-ring and a triangular screw arrangement guided by planar alignment using a digital caliper. The length from the bottom plate to the top of the pressure chamber was determined (b in Fig. 1b) and the injector holder sealed to the top of the pressure chamber. The required *x*-position of the injector holder relative to the body was found by

$$c = a + H - b \quad (1)$$

where *a* is the distance from the injector tip to the interior injector holder ring (preset to 16.1 mm); *b* is the distance from the bottom plate to the body's top surface after the first assembly step; *H* is the desired distance from the orifice to the injector tip; and *c* is the distance from the top surface of the body to the inside surface of the injector holder.

2.3. Disperse phase preparation and parameter study

The impact of selected chemical and physical parameters on microsphere generation was studied in duplicate experiments. The orifice diameter, *D*, was maintained at 100 μm for all experiments with an orifice sheet thickness, *L*, of 50 μm. Prior to microsphere generation, PLGA was dissolved in chloroform, dichloromethane, and mixtures of the two solvents at a constant polymer concentration of 10 wt%. The only exception was the evaluation of different polymer concentrations of 1, 5, 10, 15, and 20 wt% on microsphere generation with chloroform as the solvent. All parameters tested are summarized in Table 1.

2.4. Microsphere generation

All microspheres were generated using a *CP* of 2 wt% PVA solution, injected into the flow focusing apparatus using a continuous HPLC pump (Waters 501; Waters Division, Millipore, Milford, MA, USA). The *DP* consisted of chloroform or dichloromethane and was injected using a syringe pump (BS-8000; Braintree Scientific Inc., Braintree, MA, USA) and gas tight glass syringes (1000 series; Hamilton Company, Reno, NV). The experimental setup was equipped with 4-way diagonal switching valves (Upchurch Scientific, Inc., Oak Harbor, WA, USA), allowing for the switch between different disperse phase pumps without significant flow interruption. This setup allowed for purging of the *DP* injector with polymer-free solvent for 5–10 min before and between microsphere generation experiments. After establishment of stable flow conditions, the experiments were conducted by submerging the flow focusing apparatus in a beaker containing 100 ml of sterile filtered and impeller stirred (60 rpm) 2% PVA solution (Fig. 2). Micro-droplets were collected for up to 45 min to yield a theoretical dry weight of microspheres of between 8 and 10 mg per parameter studied. After the flow focusing procedure, the resulting suspension was stirred for at least two hours at room temperature to allow for solvent evaporation. The microsphere suspension was subsequently washed three times (centrifugation at 1300 × *g*, 20 min) and stored as a pellet in deionized water.

2.5. Microsphere size determination and statistical analysis

Microsphere size distribution was evaluated by microscopic methods and subsequent image analysis. Following washing and resuspension, a sample was pipetted on a microscopic slide, the particles were allowed to settle, and finally visualized using an inverted microscope (Motic AE31; Motic Instruments Inc., Richmond, BC, CAN) connected to a high resolution CCD camera (Infinity 3; Lumenera Corp., Ottawa, ON, CAN). From each parameter studied, three images were taken at different regions of a sample and analyzed by a custom coded programme (LabView Version 8.6; National Instruments Corporation, Austin, TX, USA). The programme allowed a user defined localized threshold and extracted the particle size based on edge detection and blob analysis (Fig. 2). The programme analyses the pixel values in the image and finds the edges of particles based on a specific threshold range (generally darker than the background). Each pixel is assigned a binary value (pixel value 0 for background, 1 for edges) [27]. Pixels which define an edge and are connected to form a circular pattern are found by a subroutine and the enclosed pixels are re-assigned a value of 1. Finally, the software scans the image for circular patterns with a minimum radius specified by the user. In the current analysis the minimum radius that could be detected was set to three pixels, corresponding to a minimum particle radius of 0.465 μm. This was

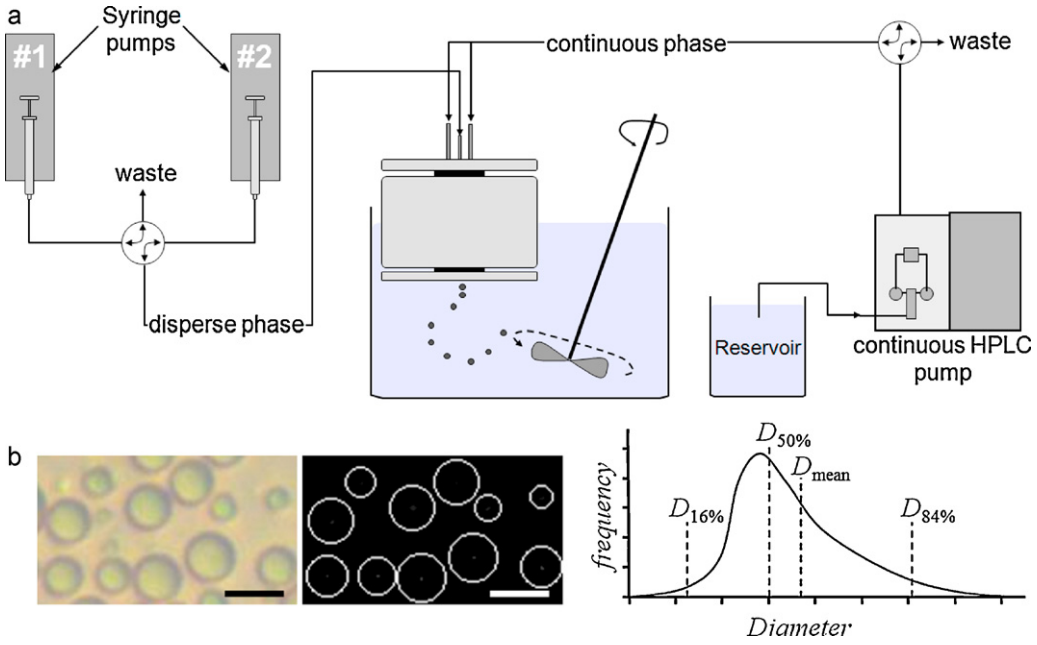

Fig. 2. (a) Flow chart of the microsphere generation procedure using syringe pumps for the *DP* and an HPLC pump for the *CP*. The flow focusing apparatus was submerged in a beaker filled with the *CP* and constantly stirred. (b) Example of a typical brightfield microscopy image of a sample and its analysis by blob analysis and edge detection (LabVIEW). Particles cropped at the edges of an image or of poor contrast (below 1 μm) were excluded from the final processing (see main text). The particle statistics are given based on the frequency distribution, arithmetic mean, and the particle diameter at the 16th, 50th, and 84th percentile (not to scale). Size bars correspond to 5 μm.

necessary to minimize the false positive tracking of particles that have poor contrast to the background of the images.

The final output of the programme was the *x*- and *y*-coordinates for each particle in the image together with the diameter. Subsequent statistics were evaluated from duplicate experiments ($n = 6$) according to DIN-ISO 9276/1-3, as density distribution and cumulative distribution functions versus the size class. The results are expressed as the 16th and 84th percentile of the cumulative size distribution representing one standard deviation from the median diameter of the sample. The particle size distribution was based on classification into 0.25 μm bins (*i.e.*, $0.25\,\mu m < x_1 \leq 0.50\,\mu m$, $0.50\,\mu m < x_2 \leq 0.75\,\mu m$, etc.). Based on this method 3000–20,000 particles were analyzed per parameter, with the lower number in batches with larger particle size distribution. If not stated otherwise, the data will be presented in the following discussion as mean particle diameter ± standard deviation ($n = 6$). Furthermore, the particle dispersion will be defined by the coefficient of variation, *CV*, which is the ratio of mean and standard deviation. A copy of the programme is available for research applications from one of the authors (TS).

3. Results and discussion

3.1. Solvent composition and polymer concentration in the disperse phase

Pharmaceutical substances, such as drugs, show different solubilities in (organic) solvents typically used in the generation of biodegradable polymer particles. The substances to be incorporated in the polymer have to be taken into account in the selection of a suitable solvent. The use of solvent mixtures, so-called co-solvents, can enhance the solubility of a pharmaceutical substance in a polymer, but may also effect the particle generation due to changes in density, viscosity, or interfacial tension [28,29]. In the current study we set out to investigate the effect of two organic solvents commonly used for (biodegradable) polymers (*i.e.*, chloroform and dichloromethane) and their different co-solvent ratios on microsphere generation.

The addition of the co-solvent chloroform to the primary PLGA solvent used in our study (dichloromethane) showed no strong effect on the particle size or its size distribution in terms of mean diameter and CV (Fig. 3). The mean particle diameter ranged from 2.67 ± 0.11 μm (100% $CHCl_3$) to 3.34 ± 0.09 μm (25% $CHCl_3$, 75% CH_2Cl_2) with a narrow range of *CV* from 0.49 to 0.62. The spread in particle size distribution (*i.e.*, $D_{84\%}$–$D_{16\%}$) is slightly decreasing with increasing concentration of chloroform in the polymer solution. This indicates that chloroform is the preferential solvent for the type of PLGA used in our study. It also shows that the use of dichloromethane as a co-solvent to enhance potential drug solubility has only a small effect on the particle size distribution.

Another parameter that affects physical properties of a polymer–solvent–drug solution is the initial polymer concentration. We investigated the change of the initial polymer concentration in the disperse phase and its effect on particle quality (*CV*, mean particle diameter). The mass throughput of microspheres generated by the flow focusing method is increasing with increasing initial polymer concentration. At the same time physical properties that affect the droplet breakup (*e.g.*, viscosity and density) are increasing. Our results indicate that with increasing polymer concentration the mean particle size distribution is increasing as well (from $CV = 0.45$ at 1% PLGA concentration to $CV = 0.69$ at 20% PLGA concentration, Fig. 3). This result suggests that a lower initial polymer concentration is beneficial for smaller particle dispersity. The reason that the lowest polymer concentration resulted in the narrowest size distribution might relate to the lower viscosity of the disperse phase prior flow focusing. A similar result was obtained in the work of Zhu et al. [30] for the preparation of PLGA microspheres using a modified w/o/w emulsion solvent evaporation technique. The group, however, did not correlate the respective viscosity values to the reduction of particle size with reducing polymer concentration in the *DP*. Similar observations for the emulsion solvent evaporation technique were presented by Grandfils et al. [31]. In the present flow focusing study, the viscosity of the 1% PLGA solution was 23 times lower than that of the 10% polymer solution (1.08 ± 0.01 mPa s compared to 23.05 ± 0.12 mPa s, $n = 3$, measured by Uebbelohde viscometry).

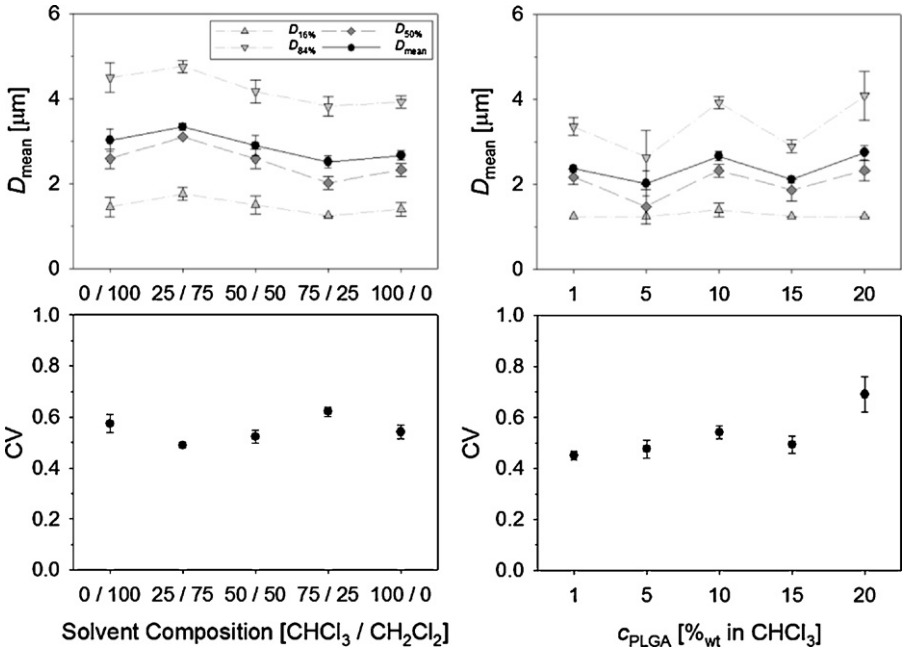

Fig. 3. Comparison of the effect of polymer solvent composition and initial polymer concentration on the microsphere size distribution. The *CV*, as well as the sphere diameters $D_{16\%}$, $D_{50\%}$ (median), $D_{84\%}$, and the arithmetic mean (±SD, $n > 3000$) are given. The total flow rate in all experiments was 8 ml/min with a flow rate ratio (Q_{DP}:Q_{total}) of 1:1000 while using a 100 μm orifice.

Lower viscosities reduce the forces necessary for droplets to break-off from the disperse phase jet at the orifice of the flow focusing device.

Overall it can be concluded, that small PLGA microspheres with low *CV* can be generated by using chloroform as the organic solvent and by keeping the initial polymer concentration as low as possible. If, however, drugs are to be encapsulated the solvent may need to be adjusted to co-dissolve both the polymer and the drug in the *DP* solvent. This will require an optimization of the solvent composition on an individual basis due to differences in solubility between the polymer and the drugs. Similarly, other materials can be encapsulated in suspended form (*i.e.*, magnetite and/or micronized drugs).

3.2. Total flow rate and flow rate ratio Q_{DP}:Q_{total}

Previous research has shown that the total flow rate has a strong impact on the size distribution of microspheres generated by the flow focusing method [32]. To investigate this effect we focused on three flow rates and four flow rate ratios that were feasible with our current experimental setup. Associated with an increase in flow rate is the increase in pressure drop along an ideal circular orifice as shown by Dagan et al. [33]:

$$\Delta P = \left(\frac{16}{\pi}\frac{L}{D} + 3\right)\frac{Q\mu}{(1/2D)^3}, \tag{2}$$

where L is the orifice thickness, D is the orifice diameter and μ is the dynamic viscosity of the *CP*. For the parameters tested in the present study (*i.e.*, $\mu_{2\%PVA} = 1.78$ mPa s, $L = 50$ μm, $D = 100$ μm), the pressure drop was approximated as being 5.28 kPa, 7.92 kPa, and 10.55 kPa for a total flow rate, Q_{total}, of 4.0 ml/min, 6.0 ml/min, and 8.0 ml/min, respectively. The mean particle diameter is decreasing in our study from 11.41 ± 1.75 μm to 2.67 ± 0.11 μm (from 4.0 ml/min to 8.0 ml/min; Fig. 4). At the same time the particle *CV* was found to be much larger for particles generated at 4.0 ml/min and 6.0 ml/min (0.90 and 0.93, respectively) than it was at 8.0 ml/min total flow rate (*CV* = 0.54). This indicates that with increasing pressure drop along the orifice in flow direction the dispersity of generated droplets will decrease. This finding is in agreement with results achieved by other groups [15]. Moreover, the trend indicates a further improvement of the statistical values for higher flow rates and, thus, a higher pressure drop. Gañan-Calvo et al. [32,34,35] showed that the monodispersity in microdroplets generated in aerodynamic flow focusing (*i.e.*, flow focusing method where gas is used as *CP*) depended on the dimensionless Weber number:

$$We = Ca \cdot Re = \frac{\rho \upsilon^2 d_j}{\gamma} = \frac{2\Delta P d_j}{\gamma}, \tag{3}$$

which in turn is directly proportional to the pressure drop across the orifice (see Eq. (2)). *Ca* and *Re* are the Capillary and Reynolds number, respectively; ρ is the density, υ is the liner flow velocity, and γ is the interfacial tension. Furthermore, a simplification to approximate the jet diameter, d_j, was introduced [15]:

$$d_j = D\sqrt{\frac{Q_D}{Q_C}} \tag{4}$$

Here, Q_D is the *DP* flow rate and Q_C is the *CP* flow rate. Based on these equations, Gañan-Calvo concluded that in aerodynamic flow focusing a stable microjet breaks into monodisperse aerosols for *We*'s between 1 and 40 [36]. However, hydrodynamic flow focusing differs from aerodynamic flow focusing due to the incompressibility of the *CP* fluid, and the use of the same *We* regimen must thus be verified. The *We*'s for the parameters investigated here are presented in Table 2. Unlike in aerodynamic flow focusing, high *We*'s do not seem to be beneficial for uniform droplet disintegration when applied to hydrodynamic flow focusing (compare Fig. 4 with Table 2). The *We* is also influenced by the jet diameter and thus by the flow rate ratio. This study indicates that with increasing total flow rate the *CV*'s are decreasing alongside with a decrease in *We* (*i.e.*, from *CV* of 0.90 and 0.93 at 4.0 and 6.0 ml/min to *CV* of 0.54 at 8.0 ml/min). More studies at higher flow rates and higher flow rate ratios are necessary to verify the trend presented in these results. With the current setup, however, the upper pumping limit for the continuous phase was reached.

Another important parameter that effects the jet size and the droplet breakup in the *DP* is the flow rate ratio and was varied

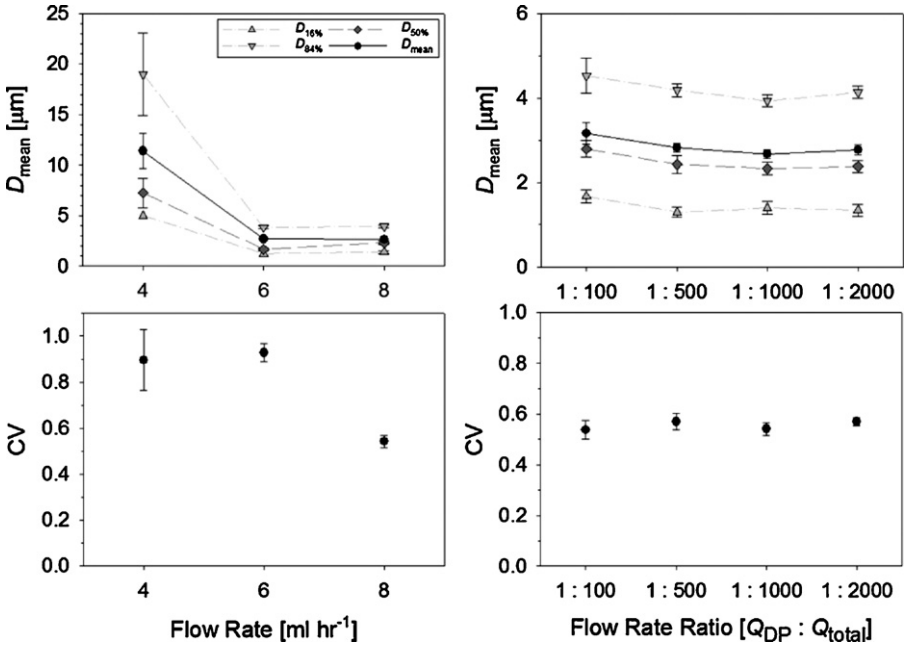

Fig. 4. Comparison of the effect of total flow rate and flow rate ratio on the microsphere formation. The *CV*, as well as the sphere diameters $D_{16\%}$, $D_{50\%}$ (median), $D_{84\%}$, and the arithmetic mean (±SD, $n > 3000$) are given. The total flow rate in all experiments was 8 ml/min with a flow rate ratio (Q_{DP}:Q_{total}) of 1:1000 while using a 100 µm orifice.

between 1:100 and 1:2000 in the current study (Fig. 4). We found that the mean particle diameter is only slightly decreasing from 3.16 ± 0.25 µm (Q_{DP}:Q_{total} = 1:100) to 2.67 ± 0.11 µm (Q_{DP}:Q_{total} = 1:1000), while the particle *CV* stayed similar (Fig. 4, Table 2). At the maximum flow rate ratio of 1:2000, the particle size opposed the overall decreasing trend in particle size. The increase in microsphere size might be attributed to the use of syringe pumps in dispensing the disperse phase. Although syringe pumps (like the Braintree Scientific BS-8000 model used in this study) can deliver rates in the µl/min range, the rates are not steady due to a pulsed motor driving the syringe screw. The number of pulses inducing the flow decreases with decreasing flow rates that are necessary to achieve a high flow rate ratio (*i.e.*, disperse phase to total flow rate). At a total flow rate of 8.0 ml/min and a flow rate ratio of 1:1000, the *DP* flow rate is 8.0 µl/min, and is induced by 37 pulses per second in an advance movement of the plunger shoe of the syringe pump. At the same total flow rate and a flow rate ratio of 1:2000 only 18 pulses per second are used (values according to manufacturers specifications for minimal advances per step). The pulsation results in flow fluctuation of the dispensed fluid and fluctuations of the prevailing pressure drop at the orifice over time and might thus produce microspheres with larger *CV*'s. This finding is in agreement with effects studied on other microfluidic devices [37]. To further improve the microsphere distributions and gain control over the size, a different method of pumping with air pressure is currently being investigated. We note that the droplet generation by flow focusing is a complex phenomenon and that the scope of the present work is not the detailed study of the droplet breakup mechanism. We were interested how changes in chemical and physical parameters effect the size distribution of biodegradable microspheres generated by hydrodynamic flow focusing. Recent studies investigated the complex interplay of parameters such as flow rate and device geometry for aerodynamic flow focusing [38]. A detailed parametric study for multiphase systems (*i.e.*, polymer–solvent solutions) with hydrodynamic flow focusing has not been conducted as to the knowledge of the authors.

Table 2
Flow rate parameters and Weber number values for the present study.

Flow rate [ml/min]	Flow rate ratio	Weber number[a]	CV
4.0	1:1000	1.09	90%
6.0	1:1000	1.64	93%
8.0	1:1000	2.19	54%
8.0	1:100	6.95	54%
8.0	1:500	3.10	57%
8.0	1:1000	2.19	54%
8.0	1:2000	1.55	57%

[a] Calculated using the published interfacial tension between disperse phase (chloroform) and continuous phase (water) of 30.5 mN/m [39].

Despite the challenges associated with continuous pumping of the *DP* at high flow rate ratios, an overall decreasing trend for all statistical microsphere parameters (*i.e.*, mean ± S.D., median, x_{16}, x_{84}, *CV*) was observed with increasing total flow rates and flow rate ratios. Hence, the improvement of microsphere generation as well as future studies aiming at encapsulating additional components into the microsphere matrix (*e.g.*, magnetite/maghemite, active components) should be conducted at higher flow rate ratios. For the present experimental setup the flow rate ratio should be 1:1000 and the total flow rate 8.0 ml/min, parameters which represent the upper and lower limit of the HPLC and syringe pumps used.

3.3. Geometric considerations

Other parameters in the flow focusing device which can be adjusted and may influence particle size distribution include the inner diameter of the *DP* injector, the orifice thickness, and the orifice diameter. By definition, the jet diameter and the droplet size after its disintegration from the bulk *DP* is proportional to the orifice diameter (Eq. (4)). Preliminary particle generation studies with a 50 µm and 25 µm orifice supported this theory (data not shown). The use of small orifice sizes for the present study, however, was found not applicable due to a significantly higher pressure drop and thus higher backpressure in the experimental system (*i.e.*, pressure chamber, tubing, and syringes). Based on Eq. (2) it can be estimated that for a given flow rate, the pressure drop at the orifice increases more than ten fold when the orifice size is reduced by a factor of 2. Specifically, for a flow rate of 8.0 ml/min, a dynamic

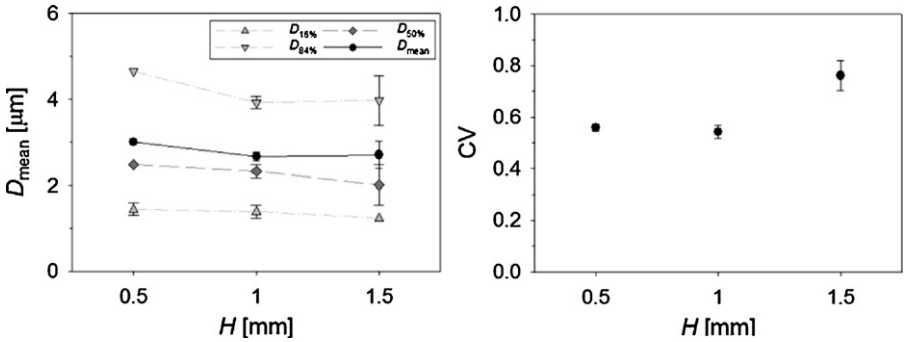

Fig. 5. Influence of the *DP* injector position relative to the orifice on the microsphere formation in terms coefficient of variation, and the sphere diameters $D_{16\%}$, $D_{50\%}$ (median), $D_{84\%}$, and the arithmetic mean (±SD, $n > 3000$). In all experiments the initial polymer concentration was 10 wt% in chloroform using a 100 μm orifice, with a total flow rate of 8 ml/min, and a flow rate ratio (Q_{DP}:Q_{total}) of 1:1000.

viscosity of the 2% PVA of 1.78 mPa s, and an orifice sheet thickness of 50 μm, the pressure drop can be approximated as 10.5 kPa, 122.9 kPa, and 1602.3 kPa for a 100 μm, 50 μm, and 25 μm orifice diameters, respectively. Thus, much lower flow rates for the *DP* would be needed, which in turn could increase the instability of the *DP* flow as discussed above. The challenges in obtaining a steady flow in the *DP* and *CP*, due to a significant reduction in total flow rate and prevailing backpressure, oppose progress in microsphere generation. Investigations with regards to backpressure and applying high flow rates are currently subject of study in our laboratory to overcome the challenges that the flow focusing technology is facing.

There are additional geometric parameters than those tested which may affect droplet disintegration and, thus, microsphere generation. To obtain a stable jet, the distance between *DP* injector tip and orifice, *H*, for example, should not exceed a critical distance. In order to evaluate the effect of misplacement of the *DP* injector in flow direction (*x*-direction), the distance *H* was varied between 0.5 mm and 1.5 mm. For the parameters tested, the optimal value for *H* (Fig. 5) was found to be 1.0 mm. An increase in *H* from 1.0 mm to 1.5 mm resulted in an increase in the *CV* from 0.54 to 0.76. At the shortest distance of *H* tested, the *CV* was similar to those found at $H = 1.00$ mm, while the mean diameter of the samples increased from 2.67 ± 0.11 μm at $H = 1.00$ mm to 3.01 ± 0.04 μm. The results from placing the injector tip further away from the orifice clearly indicate instability in the *DP* jet based on an increase in *CV* of the generated microsphere batch.

4. Conclusions

In the present parameter study, we showed the advantages and limitations of flow focusing for the continuous generation of user defined polymer microspheres. The motivation of our study was the generation of biodegradable microspheres in the challenging 1–5 μm diameter range. The results from our parameter study confirm some of the general advantages of the flow focusing method, as described for example by Martin-Banderas et al. [23]. Methods that allow the generation of uniform microspheres with a narrow size distribution in a single step and a high mass throughput are of importance for applications that employ drug loaded, biodegradable microspheres. Furthermore, other advantages of the flow focusing method include the variation in fluid and gas phases that potentially allow minimizing the stress that is applied during the particle generation procedure. This will allow the encapsulation of labile compounds and is part of a larger investigation [1]. Further advantages include the achievement of different morphologies, surface treatments and compositions that can be achieved (*e.g.*, two-phase capsules or hollow capsules); and that high particle production rates could be achieved after scaling the flow focusing geometries into two-dimensional arrays. The advantages of the technology over other established methods, such as milling, emulsification techniques, or spray drying were presented. The results indicate that the technology still poses challenges, especially in applying appropriate flow ratios, non-pulsating liquid streams, and sufficiently high throughput. These challenges are currently being addressed in our laboratory.

From the current study it can be concluded that the flow focusing method and the type of microspheres generated are strongly effected by the total flow rate. Small contributions to the spread in size distribution are given by flow rate ratios, injector position relative to the orifice, and the initial polymer concentration in the disperse phase. Minor effects were also shown with the variation of the solvent composition, which is beneficial when other substances (*i.e.*, active compounds, metals) are to be incorporated in the polymer matrix of the microsphere. Therefore, improvements to the current microsphere generation can be envisioned by improving the pumping method of both, the disperse and the continuous phase. This can be accomplished by the use of pressurized pump systems. Further improvements to increase the total throughput of microspheres could be achieved by employing arrays of flow focusing injectors placed either next to each other in one single pressure chamber or decoupled from the same continuous phase in separate stacked pressure chambers.

Acknowledgements

We appreciate the work by Bikaramjit Mann, Didier Hayem, and Berwin Song, whose preliminary efforts made these results possible, and of Shona Robinson who helped in editing this paper. Furthermore we acknowledge the support by Prof. Helen Burt and John Jackson in the Faculty of Pharmaceutical Sciences at UBC, as well as the support of Prof. Daniel T. Chiu at UW. We also are grateful for helpful discussions with Prof. Boris Stoeber and Markus Fengler in Mechanical Engineering, and Prof. Fariborz Taghipour in Chemical Engineering at UBC.

References

[1] U.O. Häfeli, K. Saatchi, P. Elischer, R. Misri, M. Bokharaei, N.R. Labiris, B. Stoeber, Biomacromolecules 11 (2010) 561.
[2] J. Castro, M. Ostoja-Starzewski, Appl. Math. Model. 24 (2000) 523.
[3] S.K. Doorn, in: J.A. Schwarz, C.I. Contescu, K. Putyera (Eds.), Encyclopedia of Nanoscience and Nanotechnology, Taylor & Francis Group Ltd., Oxford, UK, 2004, p. 3617.
[4] J.C. Giddings, Sep. Sci. Technol. 20 (1985) 749.
[5] J.C. Giddings, US Patent 4894146 (1990).
[6] P.S. Williams, S. Levin, T. Lenczycki, J.C. Giddings, Ind. Eng. Chem. Res. 31 (1992) 2172.
[7] R. Kunii, H. Onishi, Y. Machida, Eur. J. Pharm. Biopharm. 67 (2007) 9.
[8] T. Schneider, H. Zhao, J.K. Jackson, G.H. Chapman, J. Dykes, U.O. Häfeli, J. Pharm. Sci. 97 (2008) 4943.

[9] A.H. Chow, H.H. Tong, P. Chattopadhyay, B.Y. Shekunov, Pharm. Res. 24 (2007) 411.
[10] G.F. Palmieri, G. Bonacucina, P. DiMartino, S. Martelli, Drug Dev. Ind. Pharm. 21 (2001) 195.
[11] K. Ciftci, A.A. Hincal, H.S. Kas, T.M. Ercan, A. Sungur, O. Guven, S. Ruacan, Pharm. Dev. Technol. 2 (1997) 151.
[12] R. Liu, G. Ma, F.T. Meng, Z.G. Su, J. Control. Release 103 (2005) 31.
[13] C. Thomasin, H.P. Merkle, B. Gander, J. Pharm. Sci. 87 (1998) 259.
[14] O.L. Johnson, W. Jaworowicz, J.L. Cleland, L. Bailey, M. Charnis, E. Duenas, C. Wu, D. Shepard, S. Magil, T. Last, A.J.S. Jones, D.S. Putney, Pharm. Res. 14 (1997) 730.
[15] A.M. Gañan-Calvo, L. Martin-Banderas, R. Gonzalez-Prieto, A. Rodriguez-Gil, T. Berdun-Alvarez, A. Cebolla, S. Chavez, M. Flores-Mosquera, Int. J. Pharm. 324 (2006) 19.
[16] L. Rayleigh, Proc. R. Soc. London, Ser. A 29 (1879) 71.
[17] L. Rayleigh, Proc. R. Soc. London, Ser. A 28 (1879) 405.
[18] E. Bassous, L. Kuhn, A. Reisman, H.H. Taub, US Patent 4007464 (1977).
[19] W.A. Bonner, H.R. Hulett, R.G. Sweet, L.A. Herzenberg, Rev. Sci. Instrum. 43 (1972) 404.
[20] W.E. von Behrens, G.C. Oates, US Patent 3871770 (1975).
[21] P. Garstecki, A. Gañan-Calvo, G.M. Whitesides, Bull. Pol. Acad. Sci., Chem. 53 (2005) 361.
[22] I.G. Loscertales, A. Barrero, I. Guerrero, R. Cortijo, M. Marquez, A.M. Gañan-Calvo, Science 295 (2002) 1695.
[23] L. Martin-Banderas, M. Flores-Mosquera, P. Riesco-Chueca, A. Rodriguez-Gil, A. Cebolla, S. Chavez, A. Gañan-Calvo, Small 1 (2005) 688.
[24] A.B. Ripoll, A. Gañan-Calvo, I.G. Loscertales, R.C. Bon, M. Marquez, US Patent 6989169 (2006).
[25] M.A. Holgado, J.L. Arias, M.J. Cozar, J. Alvarez-Fuentes, A.M. Ganan-Calvo, M. Fernandez-Arevalo, Int. J. Pharm. 358 (2008) 27.
[26] S.H. Hyon, Yonsei Med. J. 41 (2000) 720.
[27] T. Klinger, Image Processing With LabVIEW and IMAQ Vision, Prentice Hall PTR, Upper Saddle River, NJ, 2003.
[28] K.G.H. Desai, H.J. Park, Drug Dev. Res. 62 (2004) 41.
[29] A. Rawat, D.J. Burgess, Int. J. Pharm. 394 (2010) 99.
[30] K.J. Zhu, H.L. Jiang, X.Y. Du, J. Wang, W.X. Xu, S.F. Liu, J. Microencapsul. 18 (2001) 247.
[31] C. Grandfils, P. Flandroy, N. Nihant, S. Barbette, R. Jerome, P. Teyssie, A. Thibaut, J. Biomed. Mater. Res. 26 (1992) 467.
[32] A.M. Gañan-Calvo, Phys. Rev. Lett. 80 (1998) 285.
[33] Z. Dagan, S. Weinbaum, R. Pfeffer, J. Fluid Mech. 115 (1982) 505.
[34] A.M. Gañan-Calvo, J. Fluid Mech. 335 (1997) 165.
[35] A.M. Gañan-Calvo, Phys. Rev. E Stat. Nonlin. Soft Matter Phys. 69 (2004) 027301.
[36] A. Gañan-Calvo, US Patent 6405936 (2002).
[37] P.M. Korczyk, O. Cybulski, S. Makulska, P. Garstecki, Lab Chip (2010), doi:10.1039/C0LC00088D.
[38] E.J. Vega, J.M. Montanero, M.A. Herrada, A.M. Gañán-Calvo, Phys. Fluids A 22 (2010) 064105.
[39] H. Daud, R.W. Cattrall, Aust. J. Chem. 35 (1982) 1095.